Proc. Natl. Acad. Sci. USA
Vol. 91, pp. 8842–8845, September 1994
Chemistry

Kinetic intermediates in the reactions between peptides and proteins of major histocompatibility complex class II

(antigen presentation/protein structure/reaction mechanism)

CRAIG BEESON AND HARDEN M. MCCONNELL

Department of Chemistry, Stanford University, Stanford, CA 94305

Contributed by Harden M. McConnell, June 3, 1994

ABSTRACT **The kinetics of the reactions between fluorescently labeled sperm whale myoglobin-(110–121) peptide and the murine major histocompatibility complex class II protein I-E^d have been analyzed. The presence in solution of both short- and long-lived protein–peptide complexes is demonstrated by the biphasic dissociation of the myoglobin peptide from I-E^d. The formation of the long-lived terminal complex is preceded by a characteristic induction phase. It is shown that the initially formed complex of the myoglobin peptide and I-E^d is a kinetic intermediate that undergoes a unimolecular reaction to form the terminal complex. Reactions between peptides and the class II proteins thus involve an intermediate structurally distinct from the terminal complex. The terminal complex presumably has a structure that is biologically active and similar to the published class II protein–peptide crystal structure.**

Proteins of the class II major histocompatibility complex (MHC II) present antigenic peptides to receptors on the surface of T cells. To fulfill its function, an MHC II protein must tightly bind a diverse library of peptides to ensure the eventual engagement of a cognate T-cell receptor. Crystallographic analysis of an MHC II protein bound to a single peptide has revealed a structural motif for this avid, relatively nonspecific binding—the predominant binding interactions are a series of hydrogen bonds directed toward the peptide backbone (1). Alignment of the peptide within the binding site is likely to be a cooperative process in which the energetics are sensitive to deleterious steric contacts between the peptide side chains and protein. These structural features should be reflected in the kinetics of the reactions between peptides and MHC II proteins.

Reactions between peptides and MHC II proteins have been described with a peptide-replacement reaction mechanism (2). The proteins are initially occupied with endogenous peptides; slow dissociation of these self-peptides precedes binding of an added peptide. Thus, the rate for loss of endogenous peptide is reflected in the association reaction—higher levels of occupancy are only achieved over longer time periods. The half-times ($t_{1/2}$) of formation for MHC II protein–peptide complexes increase as the peptide concentration, and thus occupancy, increases. Once formed, the complexes are often very stable with slow dissociation rates that are relatively insensitive to the peptide structure (3). However, it has been suggested recently that some peptides form unstable complexes that evade immunosurveillance and contribute to autoimmune diseases (ref. 4; K. Mason, D. W. Denney, Jr., and H.M.M., unpublished work).

Antigenic peptides restricted to a particular MHC II protein often differ in apparent affinities. The sperm whale myoglobin-(110–121) peptide (Myo) is an antigenic peptide (6) with a low apparent affinity for the murine MHC II protein I-E^d (7). For example, a 200-fold excess of the Myo peptide is required to inhibit 50% of the binding of the λ-repressor-(12–26) or hen egg white lysozyme-(105–120) (HEL) peptides to I-E^d (8). However, we have found that the amount of peptide–I-E^d complex formed with either Myo or HEL differs by only a factor of two. Further examination has revealed a biphasic dissociation of Myo from I-E^d with $t_{1/2}$ values of 15 min and 6 hr. We report here that Myo and I-E^d initially form a kinetic intermediate that undergoes a unimolecular reaction to form a terminal complex. A kinetic intermediate is not surprising, given the complexity of a published MHC II protein–peptide crystal structure (1).

MATERIALS AND METHODS

Purification of I-E^d. Detailed procedures have been described (9). Briefly, the Nonidet P-40 lysate of A20-1.11 cells was passed over a lentil lectin column that was subsequently eluted onto an affinity column derived from the monoclonal antibody 14.4.4S. The Nonidet P-40 detergent was exchanged with 1 mM n-dodecyl β-mannoside (DM), and the I-E^d was eluted from the affinity column with 1 mM DM/0.5 M NaCl/0.1 M Na_2CO_3, pH 11.5. Upon neutralization, the protein solution was dialyzed into 1 mM DM/phosphate-buffered saline (PBS) at pH 7.0 and 4°C; protein concentrations were determined with a Micro BCA assay (Pierce).

Peptide Synthesis. The peptides Myo (AIIHVLHSRHPG) and HEL (MNAWVAWRNRCKGTDV) were synthesized on an Applied Biosystems model 431A instrument with standard 9-fluorenylmethoxycarbonyl chemistry. Protected, resin-bound peptides were labeled at the N terminus with the *N*-hydroxysuccinimde ester of 5/6-carboxyfluorescein (Molecular Probes) in dimethylformamide. Both labeled and unlabeled peptides were cleaved from the resin with trifluoroacetic acid in the presence of scavengers. Peptides were purified by reverse-phase chromatography (acetonitrile/water gradient), and their identities were confirmed with high-resolution mass spectrometry.

Kinetic Analyses. Solutions of 0.1 μM I-E^d and labeled peptide in 1 mM DM/PBS/100 mM sodium citrate, pH 5.7, were incubated at 37°C. Periodically, 50- to 100-μl aliquots were removed and eluted on a small (0.7 × 3.5 cm) Sephadex G50-SF (Pharmacia) size-exclusion column with 1 mM DM/PBS, pH 7.0 at 4°C. The eluant was analyzed by high-performance size-exclusion chromatography (HPSEC) with a TosoHaas TSK SW3000 column (0.75 × 60 cm) connected to fluorescence and UV detectors in series (10). The HPSEC elutions used 1 mM DM/PBS (pH 7.0) at 1 ml·min^{-1} and

The publication costs of this article were defrayed in part by page charge payment. This article must therefore be hereby marked "*advertisement*" in accordance with 18 U.S.C. §1734 solely to indicate this fact.

Abbreviations: MHC II, major histocompatibility complex class II; Myo, a synthetic peptide corresponding to residues 110–121 of sperm whale myoglobin; HEL, a synthetic peptide corresponding to residues 105–120 of hen egg white lysozyme; f-Myo, carboxyfluorescein-labeled Myo; f-HEL, carboxyfluorescein-labeled HEL peptide; DM, *n*-dodecyl β-maltoside; HPSEC, high-performance size-exclusion chromatography.

ambient temperatures (20–23°C); the protein–peptide complex was eluted in ≈15 min. The complexes were stable at pH 7.0 relative to time required for analysis. In several experiments, a mixture of protease inhibitors (11) was added to the buffer.

For peptide-dissociation kinetics, aliquots taken from a protein–peptide incubation were eluted on the small Sephadex columns with the pH 5.7 buffer at 4°C, treated with a concentrated solution of the unlabeled peptide, and incubated at 37°C. Periodically, aliquots were removed and analyzed as described above for association kinetics. To fluorescently label I-E^d, a 4-fold excess of the *N*-hydroxysuccinimide ester of 5/6-carboxyfluorescein in dimethyl sulfoxide was added dropwise to I-E^d in 1 mM DM/PBS/100 mM $NaHCO_3$, pH 8.3, at 4°C. After 4 hr, the reaction was quenched with 1.5 M hydroxylamine, pH 8, and fluoresceinated I-E^d was purified with a Sephadex G50-SF column (1 × 15 cm) in 1 mM DM/PBS, pH 7 followed by HPSEC. Dissociation of the labeled I-E^d heterodimer into monomers was monitored by HPSEC; the α and β monomers eluted at 18 ml.

RESULTS

Kinetics of Carboxyfluorescein-Labeled Myo (f-Myo) and I-E^d Reactions. The binding of f-Myo and carboxyfluorescein-labeled HEL (f-HEL), was assayed by size-exclusion chromatography using a fluorescence detector. The affinities of the peptides are not affected by the carboxyfluorescein. An equal amount of unlabeled peptide inhibited 50% of the labeled peptide binding. The formation of f-Myo/I-E^d complexes at different peptide concentrations is illustrated in Fig. 1. The maximum amount of protein bound with 10 μM f-Myo and 10 μM f-HEL was ≈0.15 and 0.30 mole fraction, respectively. The low occupancies presumably are due to endogenous peptides that are tightly bound to the MHC II protein (12).

The rates of formation of the f-Myo/I-E^d and f-HEL/I-E^d complexes were similar ($t_{1/2}$ values from 1–10 hr). The negative slope for a plot of the $t_{1/2}$ of formation versus reciprocal peptide concentration (Fig. 1 *Inset*) is a common feature of the reaction between peptides and MHC II proteins

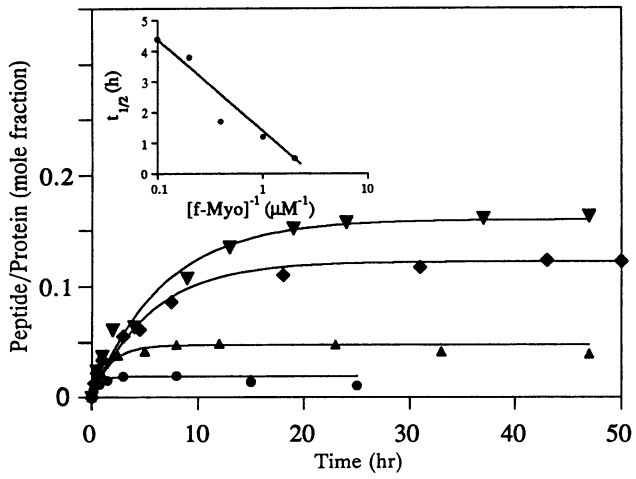

FIG. 1. Formation of the f-Myo/I-E^d complex at different peptide concentrations. Solutions of 0.1 μM I-E^d in the pH 5.7 buffer were incubated at 37°C with 0.5 μM (▲), 1 μM (●), 5 μM (◆), and 10 μM (▼) f-Myo. The mole fraction of peptide bound to protein was determined from the fluorescence of the purified complex and the protein UV absorption. The solid lines are single exponential fits to the data. As can be seen, the amount of complex formed decreases after some time at low peptide concentrations (0.5 and 1 μM f-Myo); these data points were not included in the exponential fit. The plot of the $t_{1/2}$ values versus reciprocal peptide concentration (*Inset*) was derived from the illustrated data.

(2). The slope reflects the slow rate for dissociation of endogenous peptide that precedes binding of labeled peptide. Maximum protein occupancy, achieved with high peptide concentrations, requires an extended time to allow for complete dissociation of these self-peptides. The amount of f-Myo/I-E^d complex formed in the presence of low f-Myo concentrations diminished after achieving a maximum; this was not observed at higher peptide concentrations (Fig. 1).

Solutions of I-E^d were incubated in buffer before the addition of f-Myo to assay the loss of potentially reactive MHC II protein. The maximum amount of f-Myo/I-E^d complex formed was decreased as the preincubation period was lengthened (Fig. 2). Evidently, the protein is inactivated in the absence of peptide. Dissociation of the MHC II heterodimer into α and β chains, previously reported to occur in *n*-octyl β-glucoside detergent solutions (13), has not been observed in DM solutions. The I-E^d protein itself was fluoresceinated and incubated in buffer in the absence or presence of unlabeled peptide. Dissociation of the heterodimer into monomers in the absence of peptide (data not shown) did not correlate with the loss in activity illustrated in Fig. 2. Addition of unlabeled peptide decreased the dissociation. The inactivation also occurred in the presence of protease inhibitors (11). Aggregation of the protein was not detected. Inactivation of the empty MHC II protein may be due to partial denaturation.

Dissociation of f-Myo from I-E^d is biphasic (Fig. 3); $t_{1/2}$ values of 15 min and 6 hr were obtained from a fit of the dissociation curves to a double exponential function. In contrast, dissociation of f-HEL from I-E^d is monophasic with a $t_{1/2}$ value of 23 hr (data not shown). The relative amplitudes of the two phases for the f-Myo/I-E^d dissociation reaction depended upon the time used to prepare the complex (Fig. 4). The f-Myo/I-E^d complex isolated after 4 hr of incubation with excess peptide (10 μM) had a monophasic dissociation ($t_{1/2}$ of 15 min). The more long-lived complex was initially detected after 6 hr of incubation and reached a steady-state relative amplitude of 20% by 24 hr (Fig. 4). The relative amplitudes of the two f-Myo/I-E^d dissociation phases were independent of the concentration of peptide used in the formation reaction.

Competition experiments were done to evaluate the specificity of the two subpopulations seen in the biphasic dissociation of f-Myo/I-E^d. An equal concentration of HEL inhibited >95% of the binding of f-Myo to I-E^d; a 25-fold excess

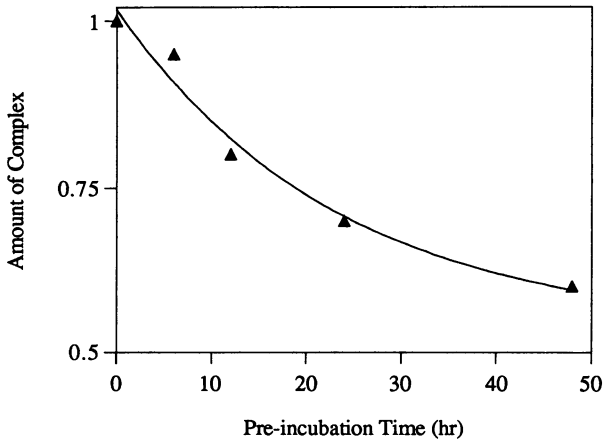

FIG. 2. Decrease in the maximum amount of I-E^d bound by f-Myo as a function of the length of preincubation. Solutions of 0.1 μM I-E^d were incubated at 37°C in the pH 5.7 buffer for different times before the addition of f-Myo (5 μM final concentration). Binding curves were obtained (as in Fig. 1), and the decrease was calculated from the steady-state amount of complex formed (20–30 hr) relative to the amount formed without preincubation. The solid line is a single exponential fit to the data ($t_{1/2}$ of 16 hr).

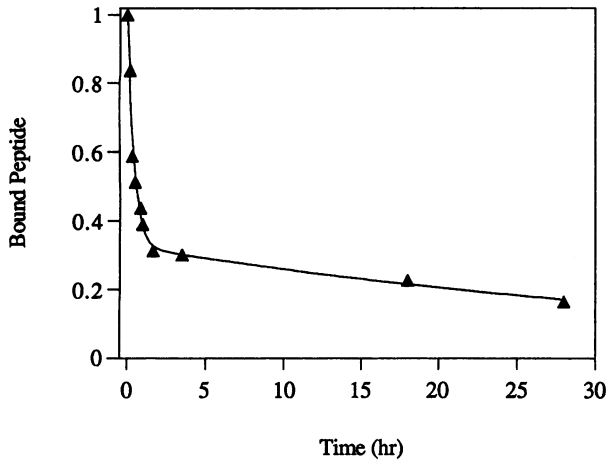

FIG. 3. Dissociation of f-Myo from I-E^d. A solution of 0.1 μM I-E^d in the pH 5.7 buffer was incubated at 37°C with 10 μM f-Myo for 24 hr. The complex was separated from excess peptide at pH 5.7 (4°C), treated with a concentrated solution of unlabeled peptide, and incubated at 37°C. The amount of complex present as a function of time was determined as described for Fig. 1. A double exponential fit to the data (solid line) gave $t_{1/2}$ values of 15 min (80%) and 6 hr (20%).

of f-Myo relative to HEL was required to recover 50% of the binding. The Myo peptide has previously been shown to be a weak competitor for HEL binding to I-E^d (7); indeed, a 10-fold excess of Myo inhibited the binding of f-HEL to I-E^d by only 20%. In either case, competition between the two peptides was similar at both early and late phases of the formation reaction (Fig. 5). The reactions of f-HEL and f-Myo with I-E^d were not inhibited by large excesses of the ovalbumin-(323–339) peptide, a nonbinding peptide for I-E^d (14).

DISCUSSION

The reaction between f-Myo and I-E^d produces both a short- and long-lived peptide–protein complex (Fig. 3). Competition by HEL confirmed that both f-Myo/I-E^d subpopulations were specific—i.e., probably bound in a cleft on the distal face of the protein (1). A mechanism that involves the

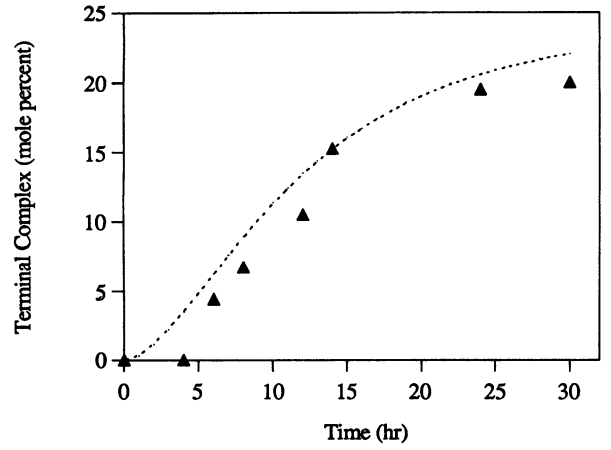

FIG. 4. Formation of the long-lived complex between f-Myo and I-E^d, expressed as the mole percent of the total amount of complex formed. Solutions of 0.1 μM I-E^d in the pH 5.7 buffer were incubated at 37°C with 10 μM f-Myo. Periodically, aliquots were removed, and the dissociation was evaluated as described for Fig. 3. The percentage of the long-lived complex was determined from the amplitudes of double exponential fits of the dissociation curves. The dashed line is from a numerical simulation of the mechanism described in text (Eqs. 1–4).

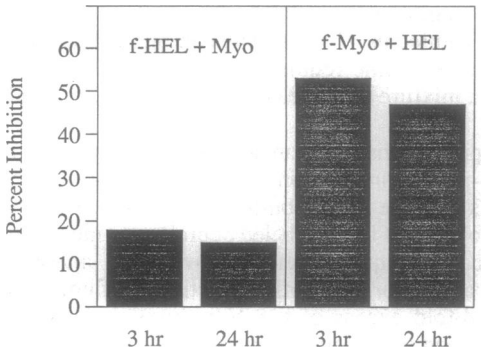

FIG. 5. Competition between Myo and HEL peptides for binding to I-E^d after 3-hr and 24-hr incubation. The percentage inhibition was calculated from the amount of complex formed in the presence of labeled and competitor peptides relative to the amount of complex formed in the absence of competitor peptide. In the reactions of f-Myo and HEL with I-E^d, the peptide concentrations were 5 μM and 0.2 μM, respectively. In the reactions of f-HEL and Myo with I-E^d, the peptide concentrations were 2 μM and 20 μM, respectively. The concentration of I-E^d was 0.1 μM.

formation of a kinetic intermediate (Eqs. 1–4) is consistent with these observations:

$$\alpha\beta P_e \underset{k_{-1}}{\overset{k_1}{\rightleftharpoons}} \alpha\beta + P_e \quad [1]$$

$$\alpha\beta + P^* \underset{k_{-2}}{\overset{k_2}{\rightleftharpoons}} \{\alpha\beta P^*\}_i \quad [2]$$

$$\{\alpha\beta P^*\}_i \underset{k_{-3}}{\overset{k_3}{\rightleftharpoons}} \alpha\beta P^* \quad [3]$$

$$\alpha\beta \xrightarrow{k_4} \alpha\beta_X. \quad [4]$$

Loss of endogenous peptide (Eq. 1) produces an empty MHC molecule that subsequently binds labeled peptide (Eq. 2) to form the kinetic intermediate; empty MHC not rescued by peptide is inactivated (Eq. 4).

The proposed mechanism (Eqs. 1–4) was simulated numerically. The inactivation of I-E^d incubated in the absence of peptide (Fig. 2) was used to estimate the ratio k_1/k_4. Because of the large excess of labeled peptide relative to the protein, terms involving k_{-1} were eliminated. The bimolecular rate constant k_2 is not experimentally accessible. However, the ratio $k_2[P^*]/k_4$ determines the onset of the inactivation phase of f-Myo/I-E^d seen at low peptide concentration (Fig. 1); the value of k_2 was adjusted to fit that behavior. The values for k_{-2} and k_{-3} were set equal to the rate constants for the rapid and slow phases of the f-Myo/I-E^d dissociations, respectively. The value for k_3 was adjusted to approximate the formation of the long-lived f-Myo/I-E^d complex (Fig. 4). The simulated formation of the two f-Myo/I-E^d complexes is illustrated in Fig. 6; parameters used for the simulation are given in Fig. 6 legend.

A critical kinetic feature apparent in the simulation of the reaction between f-Myo and I-E^d (Fig. 6) is an induction phase for production of the terminal complex. The long-lived f-Myo/I-E^d complex, experimentally assayed from the peptide dissociation, was not detected during the first 4 hr of complex formation (Fig. 4). If the long-lived complex were simply (*i*) peptide bound to a second site, (*ii*) a different peptide orientation, or (*iii*) peptide bound to a different protein, its formation would not have an induction phase. Such complexes should have been detected within the first hour of an association reaction. Thus, the long-lived species observed in the dissociation of f-Myo from I-E^d must be the product of a more rapidly formed species.

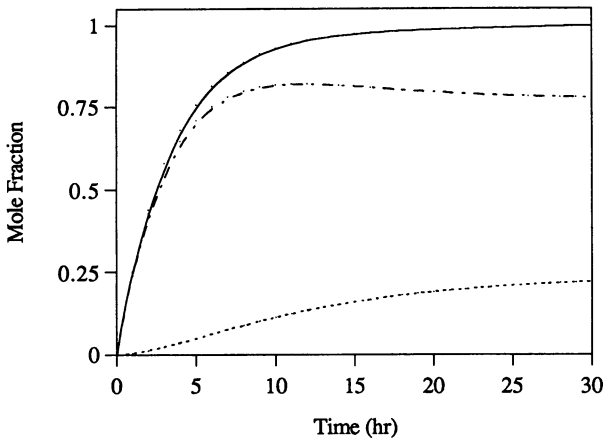

FIG. 6. Illustrative simulated binding of f-Myo to I-E^d. Shown is the mole fraction of the kinetic intermediate $\{\alpha\beta P^*\}_i$ (– · –), the terminal complex $\alpha\beta P^*$ (·····), and the sum of the two complexes (——). Differential equations for the mechanism described by Eqs. 1–4 were numerically solved with MATHEMATICA version 2.1 (Wolfram Research, Champaign, IL). Parameters used for the simulation were as follows: $k_1 = 8 \times 10^{-5}\ s^{-1}$, $k_2 = 4 \times 10^6\ M^{-1}s^{-1}$, $k_{-2} = 8 \times 10^{-4}\ s^{-1}$, $k_3 = 7 \times 10^{-6}\ s^{-1}$, $k_{-3} = 2 \times 10^{-5}\ s^{-1}$, $k_4 = 10^{-3}\ s^{-1}$, $[\alpha\beta P_e]_0 = 0.1\ \mu M$, $[P^*]_0 = 5\ \mu M$. Terms involving k_{-1} were eliminated.

The HEL peptide strongly competes with f-Myo for I-E^d and shows a 2-fold better binding. Evidently, the initial encounter between the HEL peptide and I-E^d yields a complex that dissociates slowly. The formation of a kinetic intermediate is not detected. The f-HEL peptide might form a kinetic intermediate that is not detected because it converts too rapidly to the terminal complex. Conversely, an f-HEL kinetic intermediate itself may have a very low peptide dissociation rate. It has been shown that dissociation of a truncated f-HEL peptide from I-E^d is accelerated and biphasic when the dynorphin A-(1–13) peptide is added (15). The presence of two long-lived f-HEL/I-E^d complexes for which peptide dissociation from one is promoted by dynorphin is consistent with these results (15). We suggest that the peptide in an intermediate may be susceptible to displacement by a second peptide.

It is possible that k_2 (Eq. 2), the bimolecular rate constant for peptide–protein association, does not differ substantially among peptides. Rather, it is the fate of the initially formed adduct that discriminates between peptides. The f-Myo/I-E^d intermediate rapidly loses peptide and only slowly converts to product; thus, the transient concentration of empty MHC protein is relatively high. Protein inactivation (Fig. 2) and a high transient concentration of empty protein decreases the available reservoir of protein and results in the weak loading of f-Myo and the loss of the complex at low peptide concentrations (Fig. 1). Addition of another peptide that rapidly converts empty protein to a long-lived complex produces the strong competition seen between f-Myo and HEL. The Myo peptide also forms a terminal complex with I-E^d that effectively competes with the binding of HEL after long incubations. If Myo did not form a terminal state or if the long-lived f-Myo complex were unrelated to an I-E^d binding site, it would not compete with f-HEL after long incubations (Fig. 5).

Structural transitions that might occur during the conversion of a kinetic intermediate to the terminal state are suggested by a recent structure of a peptide bound to an MHC II protein (1). The peptide is bound in an extended, twisted conformation between two α-helices and a β-sheet. A series of intermolecular hydrogen bonds extend along the peptide backbone. Perhaps the peptide initially engages some of the hydrogen bonds and then adopts the final conformation. The rate of this peptide conformational adjustment would be affected by steric interplay between the peptide side chains and protein. The protein might also require some conformational shuffling to fully accommodate the peptide side chains. Conformational transitions of MHC II proteins have been observed (16–18). Although an intermediate was not evident in the reaction with f-HEL, the structural transitions attendant to binding I-E^d are likely to be similar for both peptides.

A kinetic intermediate has also been observed in the reaction between a cytochrome *c* peptide and the murine MHC II protein I-E^k (8). Such intermediates are also suggested by discrepancies we have found between direct binding and competition for peptides that bind other murine MHC II haplotypes (data not shown). Thus, these intermediates may be general features of the reactions between peptides and MHC II proteins. Some fraction of the endogenous peptides bound to MHC II proteins may also reflect intermediate conformations. Recent experiments in this laboratory (data not shown) indicate that many peptide association rates reflect biphasic dissociation kinetics of endogenous peptides. The enhancement of MHC II protein–peptide dissociations by a second peptide (5, 15, 19) may be the result of a two-peptide complex formed between the binding peptide and a kinetic intermediate. Arguments have been advanced that rapid dissociation of myelin basic protein peptides from the MHC II molecules I-A^k and I-A^u plays a role in the induction of an autoimmune disease (ref. 4; K. Mason, D. W. Denny, Jr., and H.M.M., unpublished work). It will be of interest to determine what role intermediates play in these kinetics.

This work was supported by National Institutes of Health Grant 5R37 AI13587-17. C.B. gratefully acknowledges financial support from the Cancer Research Institute.

1. Stern, L. J., Brown, J. H., Jardetzky, T. S., Gorga, J. C., Urban, R. G., Strominger, J. L. & Wiley, D. C. (1994) *Nature (London)* **368**, 215–221.
2. Witt, S. N. & McConnell, H. M. (1993) *Acc. Chem. Res.* **26**, 442–448.
3. Witt, S. N. & McConnell, H. M. (1992) *J. Am. Chem. Soc.* **114**, 9680–9682.
4. Fairchild, P. J., Wildgoose, R., Atherton, E., Webb, S. & Wraith, D. C. (1993) *Int. Immunol.* **5**, 1151–1158.
5. Pedrazzini, T., Sette, A., Albertson, M. & Grey, H. M. (1991) *J. Immunol.* **146**, 3496–3501.
6. Ruberti, G., Sellins, K. S., Hill, M., Germain, R. N., Fathman, C. G. & Livingstone, A. (1992) *J. Exp. Med.* **175**, 157–162.
7. Sette, A., Buus, S., Colon, S., Miles, C. & Grey, H. M. (1989) *J. Immunol.* **142**, 35–40.
8. Sadegh-Nasseri, S. & McConnell, H. M. (1989) *Nature (London)* **337**, 274–276.
9. Watts, T. H., Brian, A. A., Kappler, J. W., Marrack, P. & McConnell, H. M. (1984) *Proc. Natl. Acad. Sci. USA* **81**, 7564–7568.
10. Witt, S. N. & McConnell, H. M. (1991) *Proc. Natl. Acad. Sci. USA* **88**, 8164–8168.
11. Liang, M. N., Witt, S. N. & McConnell, H. M. (1994) *J. Immunol. Methods*, in press.
12. Buus, S., Sette, A., Colon, S. M. & Grey, H. M. (1988) *Science* **242**, 1045–1049.
13. Witt, S. N. & McConnell, H. M. (1992) *J. Am. Chem. Soc.* **114**, 3506–3511.
14. Buus, S., Sette, A., Colon, S. M., Miles, C. & Grey, H. M. (1987) *Science* **235**, 1353–1358.
15. de Kroon, A. I. P. M. & McConnell, H. M. (1994) *J. Immunol.* **152**, 609–619.
16. Lee, J. M., Kay, C. M. & Watts, T. H. (1992) *Int. Immunol.* **4**, 889–897.
17. Rothenhausler, B., Dornmair, K. & McConnell, H. M. (1990) *Proc. Natl. Acad. Sci. USA* **87**, 352–354.
18. Dornmair, K., Rothenhausler, B. & McConnell, H. M. (1989) *Cold Spring Harbor Symp. Quant. Biol.* **54**, 409–416.
19. de Kroon, A. I. P. M. & McConnell, H. M. (1993) *Proc. Natl. Acad. Sci. USA* **90**, 8797–8801.